PHYSICAL REVIEW B VOLUME 47, NUMBER 16 15 APRIL 1993-II

Quantum theory of solid-state excimers: Eigenstates and transition rates

Ten-Ming Wu
Department of Physics, 0319, University of California at San Diego, La Jolla, California 92093

David W. Brown
Institute for Nonlinear Science, 0402, University of California at San Diego, La Jolla, California 92093

Katja Lindenberg
Department of Chemistry, 0340, and Institute for Nonlinear Science, 0402, University of California at San Diego, La Jolla, California 92093

(Received 14 February 1990; revised manuscript received 1 July 1991)

We present a model of excited-state dynamics in dimerized molecular crystals such as α-perylene. The essential element of the exciton-phonon interaction in this case is the modulation of resonance integrals by the relative motion of the molecules engaging in excitation transfer. Eigenstates are found for a substantial part of the model Hamiltonian and a small remainder is treated perturbatively. The eigenstates are identified with the excimer and Y states found in α-perylene, and a fit of experimental data is performed on this basis. Experimental quantities considered include Stokes shifts, Y-state lifetime, and fluorescence linewidths.

I. INTRODUCTION

In photophysical processes involving collisions of excited and unexcited molecules, it is possible for repulsive core potentials to be overcome by attractive excited-state interactions which do not exist when the same molecules are in their electronic ground states. The transient hybridization of molecular orbitals which typically occurs during molecular collision allows two-molecule excited-state orbitals to appear which have lower total energy than the separated excited and unexcited monomers. Should some agency allow surplus energy to be removed during the collision, the result can be a bound state of two molecules which exists only in an excited state—an *excited dimer,* or *excimer.*[1] In solids, collisions are replaced by lattice vibrations, and excited states by energy bands.

Excimers are distinguished by long lifetimes, Stokes shifts which are particularly large, and by a characteristic asymmetry between the shapes of absorption and emission spectra.[2–9] Absorption spectra in excimeric systems are typically narrow and structured or "monomeric," while observed emission spectra typically contain broad, structureless "excimeric" components which may dominate the usual monomeric emission.

It is perhaps another outstanding characteristic of excimers that the picture which has developed for excimers in the gas phase and in solution[10] also works very well in solids. The reason appears to be that the mutual interaction of the molecules comprising the excimer pair is so strong that the influence of the host environment amounts to only a weak perturbation. Still, there are clear indications from a number of experiments that the restrictive environment of a crystal lattice does modify excimer equilibrium configurations (e.g., relative to "free" excimers) and may in some cases inhibit excimer formation.[9]

In this context, we encounter the experimentally motivated notion of excimer precursor states. The existence of excimer precursor states is inferred from low-temperature spectral studies of a number of excimer materials wherein spectral features appear having characteristics intermediate between those of the more typical monomeric and excimeric emissions observed at higher temperatures.[11–22] At the lowest temperatures, the usual excimer emission disappears as the intermediate emission grows in strength, giving strong support to the inference that the associated state is a precursor to the excimer. For definiteness, we focus on the dimerized organic molecular crystal α-perylene, where the precursor to the excimer or "E" state has been dubbed the "Y" state.[13]

Since Tanaka[11] first observed the Y-state emission from α-perylene, a simple kinetic picture based on an asymmetric double-well potential has provided a framework within which all observations could be neatly organized. The more recent study by Walker, Port, and Wolf[18] has elaborated upon this basic picture and shown it to be satisfactory in considerable detail. While this kinetic picture provides a serviceable description of the multistage process of precursor and excimer formation and decay, it lacks a satisfactory constructive basis in terms of elementary mechanisms. A number of authors have identified the reaction coordinate implicit in the double-well picture with the intermolecular separation of the excited pair. Thus a number of anharmonic potentials have been used to model the excimer vibrational manifold.[23–26] In one recent study, for example, Dunlap and Kenkre[26] have demonstrated how a single-well anharmonic potential typical of intermolecular interactions can be deformed by a crystal field into an effective double-well potential, explicitly demonstrating the possibility that lattice inhibition of excimer formation may result in the creation of

precursor states.

We depart somewhat from this company in proposing that a satisfactory explanation of the observed characteristics of the Y and E states in α-perylene can be realized through a simple description of the linear interaction of a single excited dimer with the low-lying phonons of a dimerized lattice. We propose that the Y state is not an incompletely formed excimer, but is derived from a distinct electronic state which undergoes an activated transition to the excimer level.[27,28] This mechanism does not fall directly under the heading of lattice inhibition, and is thus complementary to inhibition mechanisms such as discussed in Ref. 26.

There is broad general agreement that the E state is derived from the symmetric pair state of the excited dimer, and that its principal characteristics can be attributed to deformation of the vibrational manifold associated with this state. We make the simple proposition that the Y state is derived from the antisymmetric state of the excited dimer, and that its principal characteristics can be similarly explained. (A similar idea has been proposed by Sumi;[29] however, it is based on electronic-state assignments quite different from ours, and leads to different results.)

Our proposal is motivated by several observations: Lattice inhibition, as commonly viewed, causes a deformation of the vibrational manifold of the excimer electronic level, and, as shown by Dunlap and Kenkre,[26] may introduce a second minimum in this manifold under appropriate conditions. While it is intuitively clear that this might lead to thermal activation and have some impact on lifetimes of the Y- and E-state emissions,[9,18,30] it is not clear (or at least has not been demonstrated) how lattice inhibition might lead to the significant isotope effect observed in the E-state emission and the essential absence of an isotope effect in the Y-state emission.[18] While it is not *necessary* that these characteristics follow from our proposed mechanism, both observations are consistent with a Y to ground-state transition which is largely allowed and an E to ground-state transition which is largely forbidden. Such a difference in selection rules would indicate a difference in symmetry in electronic states from which the Y and E states are derived.

There are other observations suggestive of such differences in symmetry. Pressure-shift data show the Y and E emissions to shift in different directions with increasing pressure.[20] Moreover, it is known that the Y state can be populated by absorption into the A_u Davydov component of α-perylene, and that the Y emission comes from a level below the A_u level and above the gerade doublet (A_g,B_g), suggesting that the Y state may be formed by relaxation from the A_u level.[14] On the other hand, the E emission comes from a level below the gerade doublet, suggesting that the E state may be formed by relaxation from these levels. Inspection of the crystal structure suggests to us that the important difference between the A_u level and those of the gerade doublet lies in the gerade/ungerade symmetry and not the A/B symmetry.[31] From this, we infer that the Y state should be identified with an antisymmetric linear combination of monomer orbitals, and that the E state should be identified with a symmetric combination.

This identification allows for the existence of Y states only in solids, since the antisymmetric state is an antibonding state and is therefore unstable in the gas phase and in solution. Should the Y and E states be derived from different electronic levels, as we propose, there would exist two electronic levels for each value of intermolecular separation. As we presently show, weakly structured, even harmonic, vibrational manifolds suffice to explain the bulk of the experimental observations, provided the coexistence of the Y- and E-state vibrational manifolds are properly accounted for. Moreover, consistent with the observations noted above, radiative transitions between the symmetric ground state and the antisymmetric excited state should be largely allowed, while radiative transitions between the symmetric ground state and the symmetric excited state should be largely forbidden.[32,33] Thus we begin with a model which is already qualitatively consistent with some of the more problematic experimental data.

We envision the following multistage absorption/emission process: (1) (largely allowed) optical absorption creates an excitation in the undeformed antisymmetric pair state; (2) fast vibrational relaxation deforms the antisymmetric pair state into the Y state; (3) the Y-state population is depleted by (largely allowed) radiative transitions to the ground state and (activated) nonradiative transitions to the E state; and (4) the E-state population is depleted by (largely forbidden) radiative transitions to the ground state.

In this paper, we focus on characterizing the Y and E states according to our interpretation, and in substantiating the thermally activated behavior we anticipate. In Sec. II, we make explicit identifications of the Y and E states, and we consider diagnostic quantities which clarify the properties of these states. In Sec. III, we derive the nonradiative transition rate from the Y to E state by means of the Fermi golden rule, and in Sec. IV we make a number of comparisons with the experimental observations of Walker, Port, and Wolf[18] for α-perylene. We summarize our conclusions in Sec. V.

II. THE MODEL

We assume that electronic excitations can transfer resonantly from one monomer to another within a given dimer, but not between dimers in distinct unit cells. We make a Born-Oppenheimer separation and assume the monomer energy levels to be functions of the instantaneous configuration $\{Q\}$ of the lattice, and the resonance integral for the excited dimer to be a function of the separation between the two monomers ΔQ. Thus the total model Hamiltonian has the form

$$H\{Q\}=E_1\{Q\}a_1^\dagger a_1+E_2\{Q\}a_2^\dagger a_2 - J(\Delta Q)(a_1^\dagger a_2+a_2^\dagger a_1)\ , \tag{2.1}$$

where $a_i^\dagger$ (a_i) creates (annihilates) an excitation on monomer i. (Here and throughout this paper, the excited dimer is assigned the cell label "0," and this label is dropped where it is not specifically needed.)

$\Delta Q \equiv Q_{01} - Q_{02}$ is the separation between the two monomers, where Q_{0i} is the position of the monomer i. Assuming that small oscillations about ground-state equilibria $\{R\}$ are sufficient to describe the desired effects, we expand $E_i\{Q\}$ and $J(\Delta Q)$ in Taylor series and truncate at linear order

$$E_i\{Q\} = E + \sum_{mj} F_{0i}^{mj}(u_{mj} - u_{0i}) + \cdots , \tag{2.2}$$

$$J(\Delta Q) = J + G(u_{01} - u_{02}) + \cdots , \tag{2.3}$$

where u_{mj} is the displacement of the jth molecule of the mth unit cell from its equilibrium position. E is the energy of an excited state of an isolated monomer, and J is the corresponding resonance integral, both evaluated when the lattice is in its ground-state equilibrium configuration. The force constants F_{ni}^{mj} and G characterize the exciton-phonon interaction; detailed definitions are given in Appendix A. Using second quantized notation for the lattice, the Hamiltonian takes the form

$$H = H_d + H_{\rm ph} + H_{\rm int} , \tag{2.4a}$$

$$H_d = E(a_1^\dagger a_1 + a_2^\dagger a_2) - J(a_1^\dagger a_2 + a_2^\dagger a_1) , \tag{2.4b}$$

$$H_{\rm ph} = \sum_{q\alpha} \hbar\omega_{q\alpha} b_{q\alpha}^\dagger b_{q\alpha} , \tag{2.4c}$$

$$H_{\rm int} = \sum_{q\alpha} \hbar\omega_{q\alpha}(b_{q\alpha}^\dagger + b_{-q\alpha})[\chi_{11}^{q\alpha} a_1^\dagger a_1 + \chi_{22}^{q\alpha} a_2^\dagger a_2 + \chi_{12}^{q\alpha}(a_1^\dagger a_2 + a_2^\dagger a_1)] , \tag{2.4d}$$

where H_d describes the electronic excited states of a dimer in the undistorted lattice, and $H_{\rm ph}$ describes the lattice vibrations. $b_{q\alpha}^\dagger$ ($b_{q\alpha}$) creates (annihilates) a phonon of mode q of branch α. $\chi_{ii}^{q\alpha}$ is the "local" coupling function for monomer i in the excited cell. In general, the local coupling functions corresponding to different lattice sites are equal in magnitude but differ by a phase factor which arises from the symmetries of the lattice. $\chi_{12}^{q\alpha}$ is the "nonlocal" coupling function.

Since the major consequences of our model depend primarily on the local geometry of the excited dimer and on the gross characteristics of the host-lattice vibrations, we can simplify our analysis by working in one dimension. Thus we take as our model lattice a dimerized harmonic linear chain having two alternating sublattice constants d and $l-d$ ($d < l-d$, cf. Fig. 1). Corresponding to these alternating sublattice constants are alternating stiffness coefficients κ_1 and κ_2 ($\kappa_1 > \kappa_2$), where κ_1 is the stiffness coefficient of the "internal" spring, and κ_2 is the stiffness coefficient of the "external" spring. The angular frequencies $\omega_{q\alpha}$ of the normal modes of a dimerized chain are then given by[34]

$$M\omega_{q\alpha}^2 = (\kappa_2 + \kappa_1) - \eta^{q\alpha}\sqrt{\kappa_2^2 + \kappa_1^2 + 2\kappa_2\kappa_1\cos(ql)} , \tag{2.5}$$

where M is the mass of a single molecule, and $\eta_1^{q\alpha}$ is $+1$ for the acoustic branch, and -1 for the optical branch. The acoustic bandwidth and the characteristic optical frequencies are given by

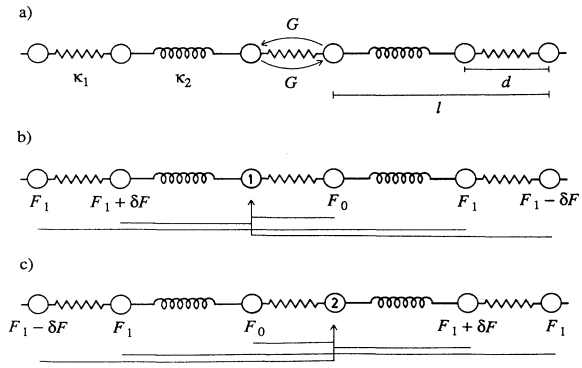

FIG. 1. Geometry of the exciton-phonon coupling. (a) κ_1 and κ_2 are the stiffness coefficients, $\kappa_1 > \kappa_2$; G is the nonlocal coupling constant; d and l are the dimer spacing in the ground state and lattice constant, $l > l-d > d$. (b) Forces affecting monomer level 1; $|F_0| > |F_1 + \delta F| > |F_1| > |F_1 - \delta F|$. (c) Forces affecting monomer level 2; while the magnitudes of corresponding forces are the same as in (b), the difference in symmetry affects the complex phases of coupling constants.

$$\omega_a = \left[\frac{2\kappa_2}{M}\right]^{1/2} , \tag{2.6a}$$

$$\omega_E = \tfrac{1}{2}(\omega_1 + \omega_2), \quad \omega_o = \tfrac{1}{2}(\omega_1 - \omega_2) , \tag{2.6b}$$

$$\omega_1 = \left[\frac{2(\kappa_2 + \kappa_1)}{M}\right]^{1/2}, \quad \omega_2 = \left[\frac{2\kappa_1}{M}\right]^{1/2} . \tag{2.6c}$$

It is well to note here that in addition to the acoustic and optical modes there are internal modes of the perylene molecule which are relevant in some respects. We do not expect internal modes to make significant contributions to either the structure of the Y and E states or the transitions between them; thus we neglect them from the bulk of our analysis. However, it is clear from experiment that such modes contribute structure to the emission line shape of the Y state, and it is possible that a similar structure is hidden beneath the broad excimer emission. Thus, when we take up the subject of emission line shapes, we will reconsider the effect of internal modes.

The detail of the exciton-phonon interaction is significantly affected by the dimerized structure of the lattice. From three "local" force constants F_0, F_1, and δF, we construct the four local forces F_0, $F_1 + \delta F$, F_1, and $F_1 - \delta F$. These forces describe the modulation of an excited monomer level by displacements of those unexcited monomers whose ground-state equilibria are found at distances d, $l-d$, l, and $l+d$, respectively, from the excited monomer. Through these three force constants, a value is assigned to each of the ten interactions linking the excimer to monomers within the excited cell and the two nearest-neighbor unit cells (cf. Fig. 1). Only one "nonlocal" force constant G is needed to describe the modulation of the resonance interaction by changes in the separation of the monomers comprising the excimer pair. The specific forms of the dimensionless coupling functions $\chi_{ij}^{q\alpha}$ appearing in (2.4) and throughout this pa-

per are derived in Appendix A.

While our model and most of the calculations which follow admit a wide range of exciton-phonon interaction strengths, we anticipate that the excimer requires values of G and F_0 much larger than F_1 and δF, since the former are derived from interactions of the two monomers comprising the excimer while the latter mediate the interaction of the excimer with its environment, an interaction which is known to be weak. G and F_0 should thus play important roles in determining the properties of the Y and E states. Phonon-induced transitions between the Y and E states will depend crucially on the value of δF; however, no gross property of the excimer appears to depend sensitively upon the value of F_1. We note that in the limit $\kappa_1 \to \infty$, the internal bond of the excimer becomes rigid, rendering F_1 the only meaningful force constant; F_1 is thus the link between properties of the excimer and properties of the well-known exciton-polaron derived from acoustic phonons and must be retained in order to maintain a complete description of the exciton-phonon interaction.

We transform the Hamiltonian (2.4) into the "Bloch representation," in which H_d is diagonal:

$$H_d = E_+ a_+^\dagger a_+ + E_- a_-^\dagger a_- , \tag{2.7a}$$

$$a_\pm = \frac{1}{\sqrt{2}}(a_1 \pm a_2) , \tag{2.7b}$$

$$E_\pm = E \mp J , \tag{2.7c}$$

a_+ ($a_+^\dagger$) annihilates (creates) a symmetric excitation of energy E_+, and a_- ($a_-^\dagger$) annihilates (creates) an antisymmetric one of energy E_-. In the Bloch representation, the exciton-phonon interaction can be decomposed into two parts,

$$H_{\rm int} = H_{\rm mod} + H_{\rm tran} , \tag{2.8a}$$

where

$$H_{\rm mod} = \sum_{q\alpha} \hbar\omega_{q\alpha}(b_{q\alpha}^\dagger + b_{-q\alpha})(\chi_+^{q\alpha} a_+^\dagger a_+ + \chi_-^{q\alpha} a_-^\dagger a_-) , \tag{2.8b}$$

$$H_{\rm trans} = \sum_{q\alpha} \hbar\omega_{q\alpha}\chi_{+-}^{q\alpha}(b_{q\alpha}^\dagger + b_{-q\alpha})(a_+^\dagger a_- + a_-^\dagger a_+) , \tag{2.8c}$$

$$\chi_\pm^{q\alpha} = \tfrac{1}{2}(\chi_{11}^{q\alpha} + \chi_{22}^{q\alpha}) \pm \chi_{12}^{q\alpha} , \tag{2.8d}$$

$$\chi_{+-}^{q\alpha} = \tfrac{1}{2}(\chi_{11}^{q\alpha} - \chi_{22}^{q\alpha}) . \tag{2.8e}$$

$H_{\rm mod}$ describes the modulation of the bare eigenstates by phonons, and $H_{\rm trans}$ describes phonon-induced transitions between the bare eigenstates.

Since the strength of the phonon-induced transitions is due to the phase asymmetry in the local coupling coefficients $\chi_{11}^{q\alpha}$ and $\chi_{22}^{q\alpha}$, we refer to the transitionless problem posed by the Hamiltonian

$$H_0 = H_d + H_{\rm ph} + H_{\rm mod} \tag{2.9}$$

as the symmetric or symmetrized case. Consulting the definitions in Appendix A, it is easily shown that χ_{+-}^{q0} is small relative to $\chi_\pm^{q0}$ under any reasonable circumstances, and χ_{+-}^{qa} is small relative to $\chi_\pm^{qa}$ provided that δF is small relative to $F_0 \pm G$ or F_1. If $\chi_{+-}^{q\alpha}$ is neglected, there are no phonon-induced transitions between the (+) and (−) states, allowing us to use the well-known displaced-oscillator transformation[35] to diagonalize H_0 in the basis of Bloch states. Thus we define the unitary transformation

$$U = \exp\left[\sum_{q\alpha}(b_{q\alpha}^\dagger - b_{-q\alpha})(\chi_+^{q\alpha} a_+^\dagger a_+ + \chi_-^{q\alpha} a_-^\dagger a_-)\right] . \tag{2.10}$$

The annihilation operators representing the new dressed quasiparticles and dressed phonons are given by

$$A_\pm = U^\dagger a_\pm U = a_\pm \exp\left[\sum_{q\alpha} \chi_\pm^{q\alpha}(b_{q\alpha}^\dagger - b_{-q\alpha})\right] , \tag{2.11a}$$

$$B_{q\alpha} = U^\dagger b_{q\alpha} U = b_{q\alpha} + (\chi_+^{q\alpha} a_+^\dagger a_+ + \chi_-^{q\alpha} a_-^\dagger a_-) . \tag{2.11b}$$

In order to maintain the distinction between these dressed quasiparticles and the more usual small polarons defined by a similar transformation in the site representation, we refer to the quasiparticles annihilated by $A_\pm$ as "Bloch polarons." We identify the (+) and (−) Bloch-polaron states with the excimer and Y states, respectively. The aim of this paper is the characterization of these states and the transitions between them.

In the Bloch-polaron basis, the symmetrized Hamiltonian takes the simple diagonal form

$$H_0 = \tilde{E}_+ A_+^\dagger A_+ + \tilde{E}_- A_-^\dagger A_- + \sum_{q\alpha} \hbar\omega_{q\alpha} B_{q\alpha}^\dagger B_{q\alpha} , \tag{2.12a}$$

where

$$\tilde{E}_\pm = E_\pm - E_\pm^{\rm bind} , \tag{2.12b}$$

$$E_\pm^{\rm bind} = \sum_{q\alpha} \hbar\omega_{q\alpha} |\chi_\pm^{q\alpha}|^2 . \tag{2.12c}$$

[A two-body term has been neglected in the Hamiltonian (2.12a), since at present we consider only one-particle states.] Although the symmetric and antisymmetric excitations put on different "phonon clothes," the dressed states retain the symmetries of the bare states from which they are derived. The symmetric and antisymmetric Bloch polarons have different binding energies, which allow the energy difference $\Delta\tilde{E}$ between these two polaron states to be greater or less than the "bare" value $2J$. In terms of the coupling coefficients in the site representation,

$$\Delta\tilde{E} = \tilde{E}_- - \tilde{E}_+ = 2J + \sum_{q\alpha} \hbar\omega_{q\alpha}(\chi_{11}^{q\alpha} + \chi_{22}^{q\alpha})\chi_{12}^{-q\alpha} . \tag{2.13}$$

We note that the deviation of $\Delta\tilde{E}$ from its bare value depends on the product of the local and nonlocal coupling coefficients, and thus depends on the *interplay* of local and nonlocal coupling.

Since our dimerized lattice has two classes of bonds, there are correspondingly two classes of bond contractions. We denote the change in the shorter "internal"

bonds $\delta D_{\pm}(m)$, and similarly denote the change in the longer "external" bonds $\Delta D_{\pm}(m)$. Thus

$$\delta D_{\pm}(m) \equiv \langle \Psi_{\pm}(0) | \hat{u}_{m2}(t) - \hat{u}_{m1}(t) | \Psi_{\pm}(0) \rangle \ , \tag{2.14a}$$

$$\Delta D_{\pm}(m) \equiv \langle \Psi_{\pm}(0) | \hat{u}_{m+1,1}(t) - \hat{u}_{m2}(t) | \Psi_{\pm}(0) \rangle \ , \tag{2.14b}$$

where $|\Psi_{\pm}(0)\rangle \equiv A_{\pm}^{+}|0\rangle$, and $\hat{u}_{mj}(t)$ is the Heisenberg operator representing the displacement u_{mj} given by

$$\hat{u}_{mj}(t) = \frac{1}{2}\left[\frac{\hbar}{MN}\right]^{1/2} \sum_{q\alpha} \frac{e^{iqml}\eta_j^{q\alpha}}{\omega_{q\alpha}^{1/2}} (b_{q\alpha}^{\dagger} + b_{-q\alpha}) \ , \tag{2.15}$$

where

$$\eta_1^{qa} = +1, \quad \eta_1^{qo} = -1 \ , \tag{2.16a}$$

$$\eta_2^{q\alpha} = \frac{\kappa_1 + \kappa_2 e^{iql}}{|\kappa_1 + \kappa_2 e^{iql}|} \ . \tag{2.16b}$$

Since the polaron states are stationary states, we find the time-independent results

$$\delta D_{\pm}(m) = \delta D_{\pm}^{a}(m) + \delta D_{\pm}^{o}(m) \ , \tag{2.17a}$$

$$\Delta D_{\pm}(m) = \Delta D_{\pm}^{a}(m) + \Delta D_{\pm}^{o}(m) \ , \tag{2.17b}$$

where $\delta D_{\pm}^{\alpha}(m)$ and $\Delta D_{\pm}^{\alpha}(m)$ are given by

$$\delta D_{\pm}^{\alpha}(m) = -\left[\frac{\hbar}{MN}\right]^{1/2} \sum_{q} \frac{e^{iqml}\chi_{\pm}^{-q\alpha}}{\omega_{q\alpha}^{1/2}} (\eta_2^{q\alpha} - \eta_1^{q\alpha}) \ , \tag{2.18a}$$

$$\Delta D_{\pm}^{\alpha}(m) = -\left[\frac{\hbar}{MN}\right]^{1/2} \sum_{q} \frac{e^{iqml}\chi_{\pm}^{-q\alpha}}{\omega_{q\alpha}^{1/2}} (\eta_1^{q\alpha} e^{iql} - \eta_2^{q\alpha}) \ . \tag{2.18b}$$

To leading order in the ratio κ_2/κ_1, we obtain the simple result

$$\delta D_{\pm}(m) \approx -\left[\frac{(F_0 \pm G) + 2F_1}{\kappa_1}\delta_{m,0} + \frac{F_1}{\kappa_1}(\delta_{m,1} + \delta_{m,-1})\right] \ , \tag{2.19a}$$

$$\Delta D_{\pm}(m) \approx -\frac{2F_1}{\kappa_2}(\delta_{m,0} + \delta_{m,-1}) \ . \tag{2.19b}$$

We note that the contraction $\delta D_{\pm}(0)$ of the "excimer bond" is determined primarily by interactions with optical phonons, while all other contractions are determined primarily by acoustic phonons. In terms of the deformation functions $\delta D_{\pm}(m)$ and $\Delta D_{\pm}(m)$, the *exact* polaron binding energies can be expressed in the intuitive form

$$E_{\pm}^{\text{bind}} = \sum_{m} \{\tfrac{1}{2}\kappa_1[\delta D_{\pm}(m)]^2 + \tfrac{1}{2}\kappa_2[\Delta D_{\pm}(m)]^2\} \ , \tag{2.20}$$

which is clearly just the net potential energy stored in all the compressed or stretched bonds of the chain. Thus it is clear that, relative to the $(-)$ state, the $(+)$ state stores "extra" energy in the "excimer bond" in the amount of

$$E_{+}^{\text{bind}} - E_{-}^{\text{bind}} = \tfrac{1}{2}\kappa_1[\delta D_{+}(0)]^2 - \tfrac{1}{2}\kappa_1[\delta D_{-}(0)]^2 \approx \frac{2G}{\kappa_1}(F_0 + 2F_1) \ , \tag{2.21}$$

which is clearly due to the cooperation/competition of local and nonlocal forces in compressing the internal bond of the excited dimer.

III. FERMI GOLDEN RULE

There are several channels through which an excitation in the Y state may decay.[18] Decay to the ground state is possible through radiative and nonradiative channels at a combined rate which we denote by k_0. Experiments on α-perylene suggest any temperature dependence of k_0 to be unimportant, so we regard k_0 as a temperature-independent constant to be determined by experiment. We denote the rate of nonradiative Y- to E-state transitions by $k_{+-}(T)$. The experimentally observed rate of decay of the Y state is thus given by

$$k(T) = k_0 + k_{+-}(T) \ . \tag{3.1}$$

We anticipate that $k_{+-}(0) \ll k_0$, so the low-temperature decay rate is essentially devoid of useful information relating to the Y- to E-state transition. The purpose of this section is to determine the temperature dependence of $k_{+-}(T)$ predicted by our model, and compare the resulting net rate $k(T)$ with experimental observations.

For a single excitation, the eigenstates of H_0 are direct products of the Bloch-polaron states and products of the dressed phonon number states. That is,

$$|\pm, \{n_{q\alpha}\}\rangle \equiv A_{\pm}^{\dagger}|0\rangle \otimes \prod_{\{n_{q\alpha}\}} \frac{B_{q\alpha}^{\dagger n_{q\alpha}}}{\sqrt{n_{q\alpha}!}}|0\rangle \ , \tag{3.2}$$

where $\{n_{q\alpha}\}$ represents a general set of phonon occupation numbers. The eigenvalues of these eigenstates are given by

$$\tilde{E}_{\pm}\{n_{q\alpha}\} = \tilde{E}_{\pm} + \sum_{q\alpha} \hbar\omega_{q\alpha} n_{q\alpha} \ . \tag{3.3}$$

The transition Hamiltonian in the dressed basis takes the form

$$H_{\text{trans}} = \sum_{q\alpha} \hbar\omega_{q\alpha}\chi_{+-}^{q\alpha}(B_{q\alpha}^{\dagger} + B_{-q\alpha}) \times (\theta_{+-}A_{+}^{\dagger}A_{-} + \theta_{-+}A_{-}^{\dagger}A_{+}) \ , \tag{3.4}$$

in which

$$\theta_{+-} = \theta_{-+}^{\dagger} = \exp\left[2\sum_{q\alpha}\chi_{12}^{q\alpha}(B_{q\alpha}^{\dagger} - B_{-q\alpha})\right] \tag{3.5}$$

is the operator which effects the rearrangement of the phonon cloud during a transition from the $(-)$ to the $(+)$ state.

Due to optical selection rules, the dimer can only be excited from the ground state, which is symmetric, to the $(-)$ state, which is antisymmetric.[32,33] The initial state is surely an essentially bare state; however, vibrational re-

laxation toward the antisymmetric Bloch-polaron state begins immediately. In organic molecular crystals such as α-perylene, typical vibrational relaxation times are of the order of a few or a few tens of picoseconds. On the other hand, the observed lifetime of the Y state in α-perylene is of the order of 10–100 ns.[18] Since vibrational relaxation times are several orders of magnitude shorter than the observed Y-state lifetime, we can safely assume that thermal equilibrium at the ambient temperature T is quickly established on the Y-state vibrational manifold.

Thus the relevant Fermi-golden-rule rate for transitions from the $(-)$ state to the $(+)$ state may be written

$$k_{+-}(T)=\frac{1}{\hbar^2}\int_{-\infty}^{\infty}dt\sum_{\{n_{q\alpha}\}}P(\{n_{q\alpha}\},T)\langle -,\{n_{q\alpha}\}|H_{\rm tran}(t)H_{\rm tran}(0)|-,\{n_{q\alpha}\}\rangle\ , \tag{3.6}$$

where $P(\{n_{q\alpha}\},T)$ denotes the thermal equilibrium probability associated with the *dressed* phonon distribution set $\{n_{q\alpha}\}$, and $H_{\rm trans}(t)$ is the transition Hamiltonian in the interaction picture; that is,

$$\begin{aligned}H_{\rm tran}(t)&=e^{iH_0t/\hbar}H_{\rm tran}e^{-iH_0t/\hbar}\\&=\sum_{q\alpha}\hbar\omega_{q\alpha}\chi_{+-}^{q\alpha}(e^{i\omega_{q\alpha}t}B_{q\alpha}^{\dagger}+e^{-i\omega_{q\alpha}t}B_{-q\alpha})[e^{-i\Delta\tilde{E}t/\hbar}\theta_{+-}(t)A_+^{\dagger}A_-+e^{i\Delta\tilde{E}t/\hbar}\theta_{-+}(t)A_-^{\dagger}A_+]\ ,\end{aligned} \tag{3.7}$$

with

$$\theta_{+-}(t)=\theta_{-+}^{\dagger}(t)=\exp\left[2\sum_{q\alpha}\chi_{12}^{q\alpha}(e^{i\omega_{q\alpha}t}B_{q\alpha}^{\dagger}-e^{-i\omega_{q\alpha}t}B_{-q\alpha})\right]\ . \tag{3.8}$$

After evaluating the required expectation values and computing the thermal average, we find

$$\begin{aligned}k_{+-}(T)=\int_{-\infty}^{\infty}dt\,e^{i\Delta\tilde{E}t/\hbar}e^{\phi(t)-\phi(0)}\sum_{q\alpha}\omega_{q\alpha}^2|\chi_{+-}^{q\alpha}|^2\{(N_{q\alpha}+1)e^{-i\omega_{q\alpha}t}+N_{q\alpha}e^{i\omega_{q\alpha}t}\\+|2\chi_{12}^{q\alpha}|^2[(N_{q\alpha}+1)(1+e^{-i\omega_{q\alpha}t})-N_{q\alpha}(1+e^{i\omega_{q\alpha}t})]^2\}\ ,\end{aligned} \tag{3.9}$$

where $N_{q\alpha}$ is the Bose distribution appropriate to $\omega_{q\alpha}$, and

$$\phi(t)=\sum_{q\alpha}|2\chi_{12}^{q\alpha}|^2[(N_{q\alpha}+1)e^{-i\omega_{q\alpha}t}+N_{q\alpha}e^{i\omega_{q\alpha}t}]\ . \tag{3.10}$$

Provided the nonlocal coupling is sufficiently strong, we can evaluate the time integral in (3.9) using a saddle-point approximation in a manner which parallels the usual polaron problem.[36,37] That is, we can rewrite $\phi(t)$ as a function of a complex argument $z=t+i\hbar\beta/2$:

$$\bar{\phi}(z)=2\sum_{q\alpha}|2\chi_{12}^{q\alpha}|^2[N_{q\alpha}(N_{q\alpha}+1)]^{1/2}\cos(\omega_{q\alpha}z)\ ; \tag{3.11}$$

$\bar{\phi}(z)$ is then expanded in a power series about the saddle point $z=0$, so that

$$\bar{\phi}(z)\approx\bar{\phi}(0)-\gamma(z/\hbar)^2+\cdots\ , \tag{3.12}$$

where

$$\gamma=\sum_{q\alpha}(\hbar\omega_{q\alpha})^2|2\chi_{12}^{q\alpha}|^2[N_{q\alpha}(N_{q\alpha}+1)]^{1/2}\ . \tag{3.13}$$

Upon truncating the series at second order in z, and deforming the integration contour to pass through the saddle point where $t=-i\beta/2$, we may carry out the time integration and obtain an approximate formula for the transition rate. The result is the somewhat cumbersome expression

$$\begin{aligned}k_{+-}(T)\approx\hbar\left[\frac{\pi}{\gamma}\right]^{1/2}e^{-[\phi(0)-\bar{\phi}(0)-\gamma\beta^2/4]}\sum_{q\alpha}\omega_{q\alpha}^2|\chi_{+-}^{q\alpha}|^2((N_{q\alpha}+1)e^{-E_{q\alpha}^2(-1)/4\gamma}+N_{q\alpha}e^{-E_{q\alpha}^2(1)/4\gamma}\\+|2\chi_{12}^{q\alpha}|^2\{(N_{q\alpha}+1)^2e^{-E_{q\alpha}^2(-2)/4\gamma}+2(N_{q\alpha}+1)e^{-E_{q\alpha}^2(-2)/4\gamma}\\+[1-2N_{q\alpha}(N_{q\alpha}+1)]e^{-E_{q\alpha}^2(0)/4\gamma}\\-2N_{q\alpha}e^{-E_{q\alpha}^2(1)/4\gamma}+N_{q\alpha}^2e^{-E_{q\alpha}^2(2)/4\gamma}\})\ ,\end{aligned} \tag{3.14}$$

where for simplicity we have introduced the notation $E_{q\alpha}(n)=\Delta\tilde{E}-\beta\gamma+n\hbar\omega_{q\alpha}$. It is this expression which has been used to fit the experimental data of Walker, Port, and Wolf.[18]

It should be noted that this approximation requires strong coupling, but does not require temperatures to be excessively high; thus the general result of this approximation may be valid over a wide range of temperatures if the coupling is sufficiently strong. To obtain a more compact and more familiar expression, we consider the limiting form of this rate found at high temperatures:

$$k_{+-}(T)\approx\Omega\left[\frac{4\pi k_B T}{\Gamma}\right]^{1/2} e^{-E_{\rm act}/k_B T}, \tag{3.15}$$

wherein

$$\Omega=\sum_{q\alpha}\omega_{q\alpha}|\chi_{+-}^{q\alpha}|^2, \tag{3.16a}$$

$$\Gamma=\sum_{q\alpha}\hbar\omega_{q\alpha}|2\chi_{12}^{q\alpha}|^2, \tag{3.16b}$$

$$E_{\rm act}=\frac{(\Delta\tilde{E}-\Gamma)^2}{4\Gamma}. \tag{3.16c}$$

One can show that in terms of the various bond contractions, the coefficient Γ can also be given as

$$\Gamma=\sum_m\{\tfrac{1}{2}\kappa_1[\delta D_+(m)-\delta D_-(m)]^2 +\tfrac{1}{2}\kappa_2[\Delta D_+(m)-\Delta D_-(m)]^2\}. \tag{3.17}$$

Because the transitions we consider are phonon assisted, the transition rate is controlled by the number of phonons present. Therefore, the prefactor is proportional to $T^{1/2}$ in the high-temperature limit, instead of the temperature dependence $T^{-1/2}$ found for intersite transitions in the usual polaron problem.[37]

In order to make clear the crucial influence of the nonlocal coupling on the transition rate, we examine the temperature dependence of the transition rate in the absence of nonlocal coupling. It is clear that (3.14) must cease to be valid when nonlocal coupling is sufficiently weak; however, in the weak nonlocal coupling limit ($G\to 0$), we can evaluate the transition rate directly from (3.9), whereupon we find the exact result

$$\lim_{G\to 0}k_{+-}(T)=2\pi\sum_{q\alpha}\hbar\omega_{q\alpha}^2|\chi_{+-}^{q\alpha}|^2 \times[N_{q\alpha}\delta(2J+\hbar\omega_{q\alpha}) +(N_{q\alpha}+1)\delta(2J-\hbar\omega_{q\alpha})]. \tag{3.18}$$

The phonon absorption term of (3.18) vanishes identically, reflecting the fact that in the absence of nonlocal coupling, those transitions from the Y state to the E state which would occur by absorbing phonons would fail to conserve the total energy. The phonon emission term of (3.18) generally contributes, but *very weakly*. The transition rate does not have an activated temperature dependence, but is linearly proportional to temperature, reflecting the fact that in the absence of nonlocal coupling there is (here) at most one phonon mode resonant with the energy gap ($2J$) separating the Y and E states. When the electronic energy gap exceeds the phonon bandwidth, one-phonon processes are forbidden, resulting in a vanishing rate. Thus it is nonlocal coupling that must be responsible for several of our system's important thermal characteristics: (1) the activated temperature dependence of the transition rate, (2) the contribution of absorptive processes, and (3) the strength of the transition.

Having these conclusions in hand, we can summarize the thermal behavior of the system in a configuration diagram. We may use the separation of the excimer pair as the reaction coordinate provided we account for the fact that the potential energy surface has two sheets. Thus we write

$$V_\pm(r)=\tilde{E}_\pm+\tfrac{1}{2}\kappa_1(r-d_\pm)^2, \tag{3.19}$$

where $d_\pm=d+\delta D_\pm(0)$. By setting $V_+(r^*)=V_-(r^*)$, the two sheets of the potential energy surface intersect at

$$r^*=\tfrac{1}{2}(d_++d_-)-\frac{\Delta\tilde{E}}{\kappa_1(d_+-d_-)}. \tag{3.20}$$

Thus, in terms of $d_\pm$ and r^*, the quantities in (3.17) are given by

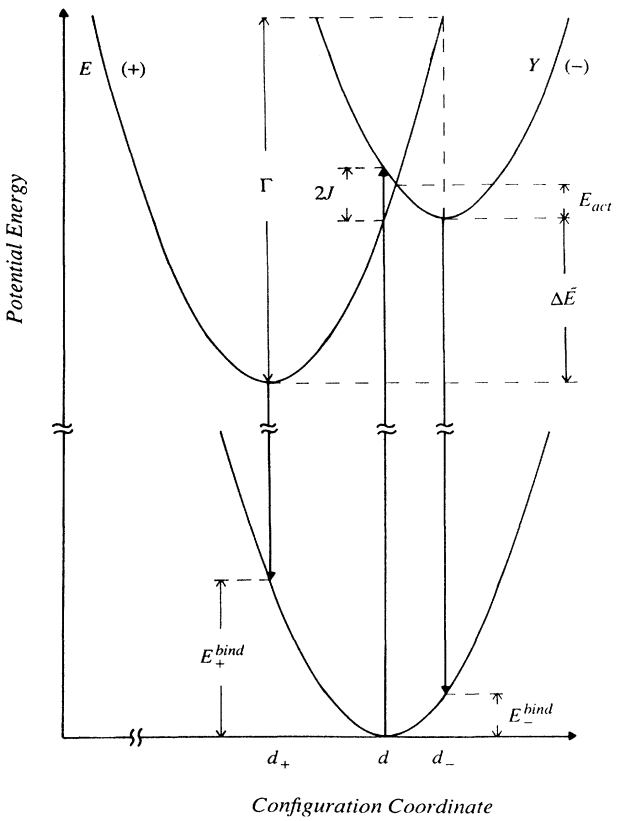

FIG. 2. Effective semiclassical potential-energy surfaces for the Y and E states. The reaction coordinate is the separation of the excimer pair.

$$\Gamma \approx \tfrac{1}{2}\kappa_1 (d_+ - d_-)^2 \tag{3.21}$$

$$E_{\rm act} = \tfrac{1}{2}\kappa_1 (r^* - d_-)^2 \ . \tag{3.22}$$

Therefore, we can draw these two sheets of the potential-energy surface as in Fig. 2, and clearly identify the activation barrier with the intersection of the Y- and E-state vibrational manifolds. This identification at once provides an explanation for the strength of the transition and the contribution of absorptive processes as well. The strength of the transition is enhanced due to the fact that in the neighborhood of r^*, the energy gap between the electronic states grows arbitrarily small, allowing *every* acoustic-phonon mode to contribute to the transition. Beyond r^*, the energy ordering of the Y and E states is reversed, allowing absorptive as well as emissive processes to contribute.

IV. COMPARISON WITH EXPERIMENT

The Y and E states of α-perylene have been studied rather extensively over a period of many years by a number of different experimental groups and by a number of techniques.[11–22] Certain measured quantities, such as lifetimes, Stokes shifts, and linewidths, have proven to be fairly robust and are generally accepted as intrinsic properties attributable to the excimer and the Y state. We now test our model by fitting our results to a suite of experimental data.

Preliminary to fitting model results, we must establish a reasonable phonon-dispersion relation. Direct measurements of the relevant dispersion relations in α-perylene appear not to be available; thus we must fix the form of the dispersion relation using less direct information. We fix the two unknowns (κ_1 and κ_2) in the dispersion relation (2.5) by assigning the Einstein frequency ω_E the value of the 104-cm^{-1} A_g mode,[38] and by assigning the longitudinal acoustic sound speed the value 2.5×10^5 cm/s found by Nelson, Dlott, and Fayer[14] along the b axis. This results in an acoustic-phonon bandwidth of approximately 25 cm^{-1}, in reasonable agreement with similar organic crystals. The width of the optical band determined in this way is a factor of 10 smaller than that of the acoustic band. The two stiffness coefficients found are quite different ($\kappa_1/\kappa_2 \approx 17$), consistent with assumptions made from time to time in the foregoing sections in order to simplify the form of presented results.

Having fixed the dispersion relation, we must adjust the four microscopic force constants G, F_0, F_1, and δF so as to obtain the best description of the basic spectral data. We do this in two stages. First, we note that in our general formula for the Y-state lifetime (3.9), the force constants F_0 and F_1 enter only through the quantity $\Delta\tilde{E}$; this quantity, however, can be obtained directly from the Stokes shifts and Davydov splitting through the relation

$$\Delta\tilde{E} = \tfrac{1}{2}(S_E - S_Y + 2J) \ , \tag{4.1}$$

where S_E and S_Y are the experimentally determined Stokes shifts for the excimer and Y states, taken to be the separation of the centroids of the absorption and emission bands. (This relation involves our model assumption that the vibrational manifolds in the ground and excited states have the same shape or curvature; this is a limiting assumption which we address below.) Thus we fit the lifetime data of Walker, Port, and Wolf[18] using only the force constants G and δF as fit parameters. In order to fit this data, however, we must recognize that the high-temperature limit (3.15) is not strictly applicable. We therefore use the more general saddle-point formula (3.14). The result of this fit is shown in Fig. 3. (The two data points at highest temperature have not been included in our fit procedure because we have been informed that the flattening out of the lifetime which these points suggest has not been borne out by later experiments. We are told that new data, not available to us at this writing, continue the downward trend without flattening out.[39]) Second, to determine F_0 and F_1, we relate the polaron binding energies to the relevant experimental Stokes shifts and the Davydov splitting:

$$E_+^{\rm bind} = \tfrac{1}{2}(S_E - 2J) \ , \tag{4.2}$$

$$E_-^{\rm bind} = \tfrac{1}{2}S_Y \ . \tag{4.3}$$

The relative values of the microscopic force constants obtained in this way are $G \approx 3\times F_0 \approx 100\times F_1, \delta F$. (Absolute values are given in Table I.)

Using these fit parameters, a number of related quantities can be calculated. We find, for example, an activation energy of 428 cm^{-1}. This is significantly higher than the 310-cm^{-1} value found by Walker, Port, and Wolf,[18] a difference which can be understood to some degree by considering the role of the temperature-dependent prefactor in our result; the corresponding prefactor in the rate formula used by Walker, Port, and Wolf[18] was temperature independent. We can also calculate the lattice distortions found in the excimer and Y states. In the excimer state, we find a bond contraction of approximately 0.35 Å. This value is in reasonable agreement with

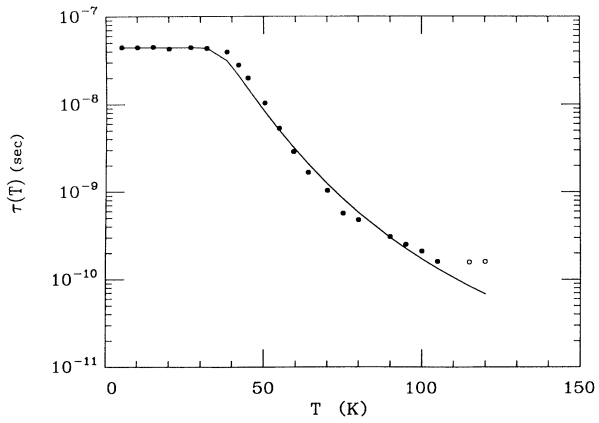

FIG. 3. The decay time of the Y fluorescence in α-perylene as a function of temperature. The solid line is the result of our model calculation. Points are experimental data from Walker, Port, and Wolf (Ref. 18); the last two points at high temperature were not included in the fitting procedure following advice of the experimentalists (Ref. 39).

Tanaka's estimate of 0.3–0.4 Å (Ref. 11) based on related but distinct considerations. In the Y state, on the other hand, we find the internal bond to be *stretched* by about half this distance.

Because the experimentally measured emission line shapes are the result of steady-state measurements, and because the vibrational relaxation times in both the Y and E states are quite long relative to the Y- to E-state transition rate and both the Y- and E-state lifetimes, we can assume thermal equilibrium conditions to hold in both the

TABLE I. *Input quantities* are those model parameters which can be determined directly from existing experimental measurements. *Derived quantities* are those model parameters which can be derived from input quantities without any knowledge of the four microscopic force constants. *Fit quantities* are the four microscopic force constants not currently accessible to direct experimental measurement; the force constants G and δF were determined by a best-fit analysis of the Y-state lifetime data of Walker, Port, and Wolf (Ref. 18), the force constants F_0 and F_1 were adjusted such that the model prediction for the binding energies agreed with values derived from the Stokes shifts (Ref. 13) and the Davydov splitting (Ref. 22). *Calculated quantities* are the model results of interest which depend on the specific values taken by the microscopic force constants and thus must be derived post-fit. *Comparison quantities* are experimental data not used in the fitting procedure, but which can be directly compared with model predictions as an independent check on the quality of the fit; the discrepancy between the comparison quantities and the calculated quantities is addressed in the text.

Quantity	Value	Source
Input quantities		
d (interplane distance)	3.47 Å	References 11 and 48
l (b axis)	10.87 Å	References 11 and 48
M	4.22×10^{-22} g	Reference 48
ω_E	104 cm^{-1}	Reference 38
v (sound speed along b axis)	2.5×10^{5} cm/s	Reference 14
$2J$	600 cm^{-1}	Reference 22
S_E (E Stokes shift)	5500 cm^{-1}	Reference 13
S_Y (Y Stokes shift)	1300 cm^{-1}	Reference 13
k_0	2.25×10^{7} s^{-1}	Reference 18
Derived quantities		
κ_2	4.72×10^{3} dyn/cm	(2.5)
κ_1	8.10×10^{4} dyn/cm	(2.5)
κ_1/κ_2	17.14	
ω_a	25.12 cm^{-1}	(2.6a)
ω_o	3.0 cm^{-1}	(2.6b)
$\Delta\tilde{E}$	2400 cm^{-1}	(4.1)
$E_+^{\text{bind}}=E_+-\tilde{E}_+$	2450 cm^{-1}	(4.2)
$E_-^{\text{bind}}=E_--\tilde{E}_-$	650 cm^{-1}	(4.3)
Fit quantities		
G	2.105×10^{-4} dyn	(3.1),(3.14)
δF	4.70×10^{-6} dyn	(3.1),(3.14)
F_0	7.60×10^{-5} dyn	(4.2),(4.3)
F_1	-2.47×10^{-6} dyn	(4.2),(4.3)
Calculated quantities		
Γ	5454 cm^{-1}	(3.16b)
E_{act}	428 cm^{-1}	(3.16c)
$\delta D_+(0)$	0.348 Å	(2.19a)
$\delta D_-(0)$	−0.176 Å	(2.19a)
FWHM (+) (at 50 K)	1233 cm^{-1}	(4.9),(4.10)
(at 300 K)	2362 cm^{-1}	
FWHM (−) (at 5 K)	598 cm^{-1}	(4.9),(4.10)
(at 50 K)	638 cm^{-1}	
Comparison quantities		
FWHM (+) (at 50 K)	1900 cm^{-1}	Reference 18
(at 300 K)	3500 cm^{-1}	Reference 18
FWHM (−) (at 5 K)	1000 cm^{-1}	Reference 13
(at 50 K)	1000 cm^{-1}	Reference 13

Y- and E-state vibrational manifolds for the purpose of calculating emission spectra.

In order to address the full structure of the emission line shapes, however, we must briefly consider the internal modes of the perylene molecule. Provided the internal and external modes of vibration are weakly correlated, the complete emission spectrum should be well represented by the convolution of the fundamental spectra $F_{\pm}(\omega)$ due to crystal modes, and the monomer spectrum $M(\omega)$ due to internal modes

$$I_{\pm}(\omega)\approx\frac{1}{2\pi}\int_{-\infty}^{+\infty}d\omega' F_{\pm}(\omega-\omega')M(\omega') \ . \tag{4.4}$$

The monomer spectrum, of course, is itself an extended convolution of contributions from all the internal modes of vibration; however, one or two dominant contributions suffice to give its approximate shape. For example, the main peak of the Y emission and the few peaks resolved on its low-energy side are separated by approximately $\hbar\omega_M=1350\ \text{cm}^{-1}$, in good correspondence with one of the known internal modes of perylene.[40,41] (The peak on the high-energy side of the main peak suggests a contribution from a second internal mode which, for simplicity, we do not consider. See Sumi[29] for a more extended discussion.) Since $\hbar\omega_M$ is high relative to k_BT even at room temperature, we do not need to consider thermal population factors, allowing the monomer spectrum to be given simply as

$$M(\omega)=M_0\sum_{l=0}\frac{g^l}{l!}\delta[\omega-(l+g)\omega_M] \ , \tag{4.5}$$

where g is a constant related to the coupling strength of the intramolecular mode;[37] this constant can be determined from the experimental spectra to be approximately 0.3 for the case of interest here.

To calculate the fundamental spectrum, we use the methods of the previous sections; thus,

$$F_{\pm}(\omega)\approx\frac{2\pi}{\hbar^2}|\mu_{\pm}|^2\int_{-\infty}^{+\infty}dt\, e^{-i(\hbar\omega-\bar{E}_{\pm})t/\hbar}e^{-\phi_{\pm}(t)} \ , \tag{4.6}$$

where

$$\phi_{\pm}(t)=\sum_{q\alpha}|\chi_{\pm}^{q\alpha}|^2[(N_{q\alpha}+1)e^{-i\omega_{q\alpha}t}+N_{q\alpha}e^{i\omega_{q\alpha}t}] \ . \tag{4.7}$$

Since both the excimer and Y emissions are very nearly Gaussian, we may expand $\phi_{\pm}(t)$ to second order in time and use the resulting Gaussian integral to approximate the line shape.[42] Thus

$$F_{\pm}(\omega)\approx\frac{(2\pi)^{3/2}}{\hbar}|\mu^{\pm}|^2\frac{1}{\sigma_{\pm}}\times\exp\left\{-\frac{[\hbar\omega-(E_{\pm}-2E_{\pm}^{\text{bind}})]^2}{2\sigma_{\pm}^2}\right\} \ , \tag{4.8}$$

$$\sigma_{\pm}^2=\sum_{q\alpha}|\chi_{\pm}^{q\alpha}|^2\hbar^2\omega_{q\alpha}^2\coth(\tfrac{1}{2}\beta\hbar\omega_{q\alpha}) \ . \tag{4.9}$$

The result of convoluting this approximate fundamental spectrum with the approximate monomer spectrum is shown in Fig. 4. The parameter values used in obtaining the displayed line shapes are the same values determined by our fit of the transition rate data and Stokes shifts. It should be noted that these parameters are determined once for all temperatures, so the changes in line shape seen in Fig. 4 reflect intrinsic properties of the theory and are not the result of independent fits at different temperatures.

Our calculated line shapes are narrower than the observed lines by a significant fraction. The full width at

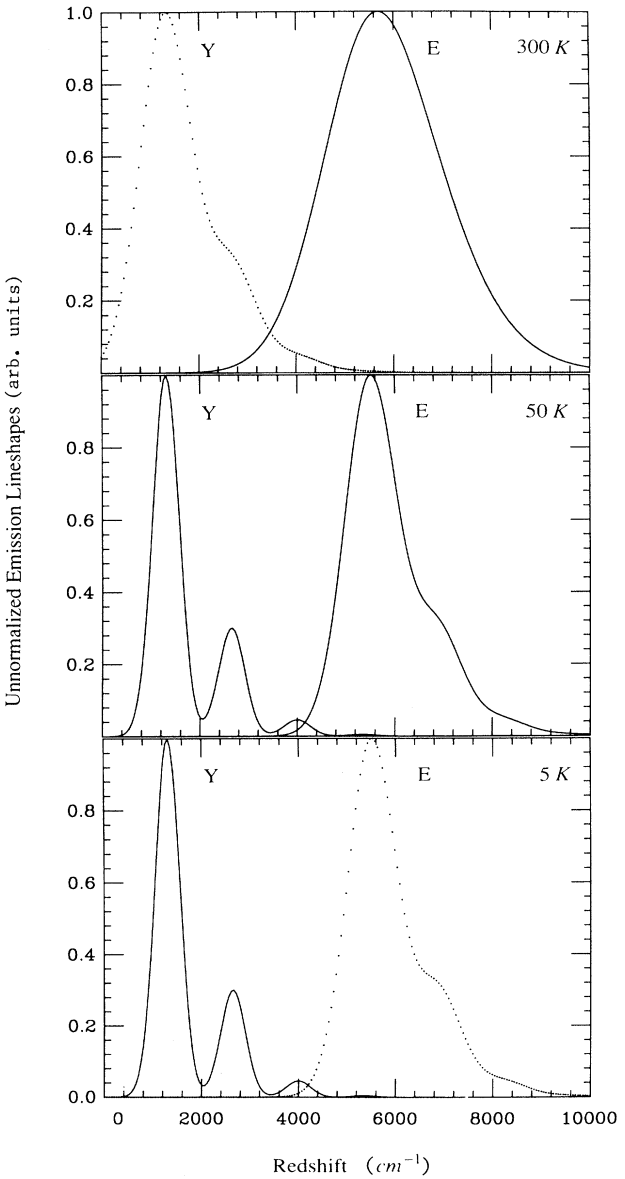

FIG. 4. Emission spectra as calculated from (4.4) ff. Each panel represents a different temperature; (a) $T=300$ K, (b) $T=50$ K, and (c) $T=5$ K. In consideration of the fact that our approximate method does not allow the accurate determination of total intensities, the height of the main peak of each emission spectrum has been arbitrarily set to unity. Solid curves indicate the predicted shapes of lines actually observed; dotted curves indicate the predicted shapes of lines too weak to be resolved in experiments reported thus far.

half maximum (FWHM) given in terms of the Gaussian dispersion is

$$\text{FWHM}(\pm)=2\sqrt{2\ln 2}\,\sigma_{\pm}\ . \tag{4.10}$$

The absolute values of the FWHM thus obtained (cf. Table I) are smaller than the measured values by roughly one third; this factor appears *uniformly* in that the same factor applies very nearly to both the excimer width and Y-state width, and at all measured temperatures, suggesting that the source of the discrepancy may lie in a single scale factor. That there should be such a factor might have been anticipated, based on a comparison of our method with the previous analysis of Birks and Kazzaz[43] applied to pyrene. These authors considered the decay of an extinction from a single shifted harmonic vibrational manifold, and concluded that the ground-state manifold should be significantly "stiffer" than that of the excited state in order to account for the full width of the excimer emission. In our approach, the vibrational manifolds in the ground and excited states have the same shape, a fact we have exploited to obtain simple and exact solutions. We expect that a modest generalization of our method which would allow for a softer internal spring constant in the excited state would make up for the noted deficit in width. Preliminary results of such a generalization suggest that a comparable analysis is possible;[44] however, reportable results are not yet available.

V. CONCLUSION

In this paper, we have attempted to render plausible a possible mechanism for occurrence of excimer and Y states in dimerized solids such as α-perylene. While other mechanisms may also be considered plausible, we find our proposal compelling for the simple reason that the effects we identify follow necessarily from the most elementary interactions which must be present in the relevant lattice geometry; we require no exotic or special effects in order to arrive at a satisfactory explanation of the available spectral data. Indeed, viewed from an appropriate perspective, our proposal is almost prosaic.

If all that we suggest is true, one should immediately ask two questions: First, why is the observation of excimer and Y states not the rule in all dimerized solids; and second, is our proposal limited to dimerized solids and therefore not applicable to simpler solids, where the dimerized lattice structure does not appear to play any role? Regarding the first question, it is clear from our analysis that distinct excimer and Y states should be found only when nonlocal coupling as measured by G is significant relative to local coupling as measured by F_0, and this crucial property is not guaranteed by the mere existence of a dimerized lattice structure. We should not, therefore, expect excimers and Y states to appear routinely in dimerized solids, but incidentally in those solids where nonlocal coupling is strong. Regarding the second question, almost the same answer applies: it seems likely to us that the dimerized structure of the lattice is a convenience and not a necessity. The crucial element of the proposed mechanism lies in the fact that nonlocal coupling is quite sensitive to excited-state symmetry. In a generic lattice, where normal energy-band transport is expected in the absence of interactions with phonons, our eigenstate label $(\pm)$ generalizes to the wave vector k. The wave vector, of course, is a symmetry label like our $(\pm)$; typically, states near one edge of an energy band are nearly antisymmetric like our $(-)$ state, and states near the other edge of the band are nearly symmetric like our $(+)$. Generalizing our conclusions, one might expect excimerlike states near one edge of a band and Y-like states near the other. Since excimer and Y states typically experience different kinds of energy shifts, one might expect energy shifts to vary across the band, leading to phonon-induced distortions of the energy band in materials where this mechanism is operative. This is precisely what has been found previously in related studies by Dissado and Walmsley[45,46] and by Munn and Silbey.[47]

Our proposal allows us to account for important excimer and Y-state characteristics such as Stokes shifts, relative linewidths, the activated nature of the Y- to E-state transition, and the detail of the temperature dependence of the transition rate. In addition, selection rules which one would expect to apply make the model qualitatively consistent with accessory observations of isotope effects in decay rates. One detail which does not yet fall in line with experimental observations is the absolute value of the fluorescence linewidth; our results still show a deficit in linewidth. As noted above, this detail appears to be due to greater softness in the excited-state vibrational manifolds than in the ground state. We expect this defect to be remedied within a generalized model;[44] however, it must be noted that one should expect the specific values of the fit parameters to change somewhat in the course of generalization. In consideration of this, and the fact that we have approximated the four Davydov components of α-perylene by only two levels, and have replaced the three-dimensional α-perylene crystal lattice by a one-dimensional harmonic chain, what is most meaningful about these specific-fit parameters is not their absolute values but their relative magnitudes; perforce, it should be noted that throughout our fitting procedure, and under many trial assumptions (including the use of synthetic, noisy data to test the sensitivity of our fits to modest random errors), the relative values of the best-fit elementary force constants were roughly maintained. The fact that a satisfactory fit of the α-perylene data should require such a large relative strength of the nonlocal exciton-phonon interaction is perhaps the most significant single observation for future modeling considerations.

Note added in proof. Since the original submission of this paper, there have been several developments worth noting.

(1) Neutron-scattering experiments mapping out the phonon-dispersion relation for α-perylene have been reported by Schliefer *et al.* in Ref. 49. The bandwidth of longitudinal-acoustic phonons according to these measurements is somewhat greater than 20 cm^{-1}, in reasonable agreement with the estimated value of 25 cm^{-1} used in this paper.

(2) The conjecture at the end of Sec. IV that the one-third deficit in linewidth we find in this paper might be

made up by explicitly accounting for a suspected softness in the excited bond has been borne out in our analysis of a generalized model to be presented elsewhere.[50] That analysis involves the formation of a local vibrational mode on the excimer bond, and a renormalization of all related quantities.

(3) Spectroscopic studies of perylene monolayers in Langmuir-Blodgett films have produced results consistent in many respects with the model presented here.[51,52] However, those experiments raise a number of difficult questions which challenge all existing analyses of α-perylene, including the one presented here. Continued study of this problem from a sufficiently general perspective is required.

ACKNOWLEDGMENTS

This work was supported in part by the U.S. Defense Advanced Research Projects Agency under ARPA Order 7048, and by the National Science Foundation under Grant No. DMR 86-19650-A1.

APPENDIX A

In this Appendix, we derive the coupling constants from a specific model of exciton-phonon coupling in a dimerized chain. We make a number of assumptions in order to obtain wieldable results; however, all of the essential features of interplay of the exciton-phonon interaction with the geometry of the lattice are preserved. We assume that only motions within a given unit cell and interactions between contiguous unit cells are of importance. In this approximation, the force tensor F_{ni}^{mj}, given by

$$F_{ni}^{mj} \equiv \left. \frac{\partial E_{ni}\{Q\}}{\partial Q_{mj}} \right|_{\{Q\}=\{R\}} , \tag{A1}$$

has ten relevant nonvanishing elements indicated in Fig. 1:

$$F_{01}^{02} = -F_{02}^{01} = F_0 , \tag{A2a}$$

$$F_{01}^{11} = -F_{01}^{-11} = F_{02}^{12} = -F_{01}^{-12} = F_1 , \tag{A2b}$$

$$F_{02}^{11} = -F_{01}^{-12} = F_1 + \delta F , \tag{A2c}$$

$$F_{01}^{12} = -F_{02}^{-11} = F_1 - \delta F . \tag{A2d}$$

F_0 is the force constant giving the energy shift of an isolated monomer level due to a unit displacement of the unexcited monomer in the same excimer pair. F_1 is the force constant giving the energy shift of an isolated monomer level due to a unit displacement of an unexcited monomer occupying an identical position in one of the two nearest-neighbor unit cells. In a reasonable approximation, the force constants characterizing the remaining interactions between the constituents of nearest-neighbor unit cells can be taken to be $F_1 \pm \delta F$, with (+) corresponding to the nearest and (−) to the farthest pairs of monomers in nearest-neighbor cells. We refer to all such "F" forces as "local" forces, and we shall find that all three force constants F_0, F_1, and δF are essential to describe the excimer. On the other hand, to describe modulation of the resonance integral, we need consider only changes in the separation of the monomers comprising the excimer pair; thus we require only one force constant,

$$G \equiv \left. \frac{\partial J\{Q\}}{\partial Q_{01}} \right|_{\{Q\}=\{R\}} = - \left. \frac{\partial J\{Q\}}{\partial Q_{02}} \right|_{\{Q\}=\{R\}} , \tag{A3}$$

which we refer to as a "nonlocal" force.

The dimensionless coupling functions $\chi_{ij}^{q\alpha}$ are given by

$$\chi_{11}^{q\alpha} = \left[\frac{1}{\hbar M N \omega_{q\alpha}^3} \right]^{1/2} \left[\frac{F_0}{2} (\eta_2^{q\alpha} - \eta_1^{q\alpha}) + iF_1 \sin(ql)(\eta_2^{q\alpha} + \eta_1^{q\alpha}) - \delta F [\cos(ql)\eta_2^{q\alpha} - \eta_1^{q\alpha}] \right] , \tag{A4}$$

$$\chi_{22}^{q\alpha} = \left[\frac{1}{\hbar M N \omega_{q\alpha}^3} \right]^{1/2} \left[\frac{F_0}{2} (\eta_2^{q\alpha} - \eta_1^{q\alpha}) + iF_1 \sin(ql)(\eta_2^{q\alpha} + \eta_1^{q\alpha}) - \delta F [\eta_2^{q\alpha} - \eta_1^{q\alpha} \cos(ql)] \right] , \tag{A5}$$

$$\chi_{12}^{q\alpha} = \left[\frac{1}{\hbar M N \omega_{q\alpha}^3} \right]^{1/2} \left[\frac{G}{2} (\eta_2^{q\alpha} - \eta_1^{q\alpha}) \right] , \tag{A6}$$

where the $\eta_j^{q\alpha}$ are defined in (2.16). In the basis of Bloch states, the coupling functions take the form

$$\chi_{\pm}^{q\alpha} = \left[\frac{1}{\hbar M N \omega_{q\alpha}^3} \right]^{1/2} \{ [\tfrac{1}{2}(F_0 \pm G) - \delta F \cos(\tfrac{1}{2}ql)](\eta_2^{q\alpha} - \eta_1^{q\alpha}) + iF_1 \sin(ql)(\eta_2^{q\alpha} + \eta_1^{q\alpha}) \} , \tag{A7}$$

$$\chi_{+-}^{q\alpha} = \left[\frac{1}{\hbar M N \omega_{q\alpha}^3} \right]^{1/2} \delta F (\eta_1^{q\alpha} + \eta_2^{q\alpha}) \sin^2(\tfrac{1}{2}ql) . \tag{A8}$$

Keeping in mind the anticipated relative magnitudes $\kappa_1 \gg \kappa_2$ and G, $F_0 \gg F_1, \delta F$, (A7) shows that the (+) and (−) state characteristics are predominantly determined by interactions with optical phonons; however, (A8) shows that the transitions between these states are predominantly determined by interactions with acoustic phonons. These expectations are borne out by detailed calculations such as those in the main text.

[1] B. Stevens and E. Hutton, Nature **186**, 1045 (1960).

[2] *Modern Quantum Chemistry, Part III: Action of Light and Organic Crystals,* edited by Oktay Sinanoglu (Academic, New York, 1965).

[3] Th. Forster, Angew. Chem. Intern. Ed. **8**, 333 (1969).

[4] J. B. Birks, *Photophysics of Aromatic Molecules* (Wiley-Interscience, New York, 1970).

[5] *Organic Molecular Photophysics,* edited by J. B. Birks (Wiley,

New York, 1975), Vols. 1 and 2.
[6]*The Exiplex,* edited by M. Gordon and W. R. Ware (Academic, New York, 1975).
[7]N. J. Turro, *Modern Molecular Photochemistry* (Benjamin/Cummings, Reading, MA, 1978).
[8]Mendel D. Cohen, Mol. Cryst. Liq. Cryst. **50**, 1 (1979).
[9]V. Yakhot, M. D. Cohen, and Z. Ludmer, Adv. Photochem. **11**, 489 (1979).
[10]B. Stevens and M. I. Ban, Trans. Faraday Society **60**, 1515 (1964).
[11]J. Tanaka, Bull. Chem. Soc. Jpn. **36**, 1237 (1963).
[12]J. Tanaka, T. Kishi, and M. Tanaka, Bull. Chem. Soc. Jpn. **47**, 2376 (1974).
[13]E. Von Freydorf, J. Kinder, and M. E. Michel-Beyerle, Chem. Phys. **27**, 199 (1978).
[14]K. A. Nelson, D. D. Dlott, and M. D. Fayer, Chem. Phys. Lett. **64**, 88 (1979).
[15]H. Auweter, D. Ramer, B. Kunze, and H. C. Wolf, Chem. Phys. Lett. **85**, 325 (1982).
[16]H. Port, B. Walker, and H. C. Wolf, J. Lumin. **31&32**, 780 (1984).
[17]H. Port, R. Seyfang, and H. C. Wolf, J. Phys. (Paris) Colloq. **46**, C7-391 (1985).
[18]B. Walker, H. Port, and H. C. Wolf, Chem. Phys. **92**, 177 (1985).
[19]R. Seyfang, E. Betz, H. Port, W. Schrof, and H. C. Wolf, J. Lumin. **34**, 57 (1985).
[20]K. Mizuno and A. Matsui, J. Mol. Electron. **4**, 187 (1985).
[21]R. Seyfang, H. Port, and H. C. Wolf, J. Lumin. **42**, 127 (1988).
[22]A. Matsui, T. Ohno, K. Mizuno, T. Yokoyama, and M. Kobayashi, Chem. Phys. **111**, 121 (1987).
[23]M. D. Cohen and V. Yakhot, Chem. Phys. **5**, 27 (1974).
[24]M. A. Collins and D. P. Craig, Chem. Phys. **54**, 305 (1981).
[25]D. H. Dunlap and V. M. Kenkre, Chem. Phys. **105**, 51 (1986).
[26]D. H. Dunlap and V. M. Kenkre, Phys. Rev. B **34**, 4390 (1988).
[27]Ten-Ming Wu, David W. Brown, and Katja Lindenberg, J. Lumin. **45**, 245 (1990).
[28]Ten-Ming Wu, David W. Brown, and Katja Lindenberg, in *Davydov's Soliton Revisited: Self-Trapping of Vibrational Energy in Protein,* Vol. 243 of *NATO Advanced Study Institute Series B: Physics,* edited by Peter Christiansen and Alwyn C. Scott (Plenum, New York, 1990).
[29]H. Sumi, Chem. Phys. **130**, 433 (1989).
[30]M. D. Cohen, R. Haberkorn, E. Huler, Z. Ludmer, M. E. Michel-Beyerle, D. Rabinovich, R. Sharon, A. Warshel, and V. Yakhot, Chem. Phys. **27**, 211 (1978).
[31]R. M. Hochstrasser, J. Chem. Phys. **40**, 2559 (1964).
[32]M. Kasha, Rad. Res. **20**, 55 (1963).
[33]C. A. Hunter, J. K. M. Sanders, and A. J. Stone, Chem. Phys. **133**, 395 (1989).
[34]N. W. Ashcroft and N. D. Mermin, *Solid State Physics* (Holt, Rinehart and Winston, New York, 1976).
[35]I. G. Lang and Yu. A. Firsov, Zh. Eksp. Teor. Fiz. **43**, 1843 (1962) [Sov. Phys. JETP **16**, 1301 (1963)].
[36]K. D. Schotte, Z. Phys. **196**, 393 (1966).
[37]G. D. Mahan, *Many-Particle Physics* (Plenum, New York, 1981), p. 534.
[38]T. J. Kosic, C. L. Schosser, and D. D. Dlott, Chem. Phys. Lett. **57**, (1983).
[39]H. Port (private communication).
[40]E. V. Shpol'skii and R. I. Personov, Opt. Spectrosc. **8**, 172 (1960).
[41]M. M. Valdman and R. I. Personov, Opt. Spectrosc. **19**, 296 (1965).
[42]S. Nakajima, Y. Toyozawa, and R. Abe, in *The Physics of Elementary Excitations,* edited by M. Cardona, P. Fulde, and H.-J. Queisser, Springer Series in Solid-State Sciences Vol. 12 (Springer-Verlag, Berlin, 1980).
[43]J. B. Birks and A. A. Kazzaz, Proc. R. Soc. London Ser. A **304**, 291 (1968).
[44]Ten-Ming Wu, David W. Brown, and Katja Lindenberg (unpublished).
[45]L. A. Dissado and S. H. Walmsley, Chem. Phys. Lett. **87**, 74 (1982).
[46]L. A. Dissado and S. H. Walmsley, Chem. Phys. **86**, 375 (1984).
[47]R. W. Munn and R. Silbey, J. Chem. Phys. **83**, 1843 (1985).
[48]D. M. Donaldson, J. M. Robertson, and J. G. White, Proc. R. Soc. London Ser. A **220**, 311 (1953).
[49]J. Schleifer, J. Kalus, U. Schlmelzer, and G. Eckold, Phys. Status Solidi B **154**, 153 (1989).
[50]Ten-Ming Wu, David W. Brown, and Katia Lindenberg (unpublished).
[51]D. Weiss, R. Kietzmann, J. Mahrt, B. Tufts, W. Storck, and F. Willig, J. Phys. Chem. **96**, 5320 (1992).
[52]Dietmar Weiss, Ph.D. thesis, The Technical University of Berlin, 1992.